Engineering Solid Mechanics12 (2024) 237-246

Contents lists available at GrowingScience

Engineering Solid Mechanics

homepage: www.GrowingScience.com/esm

Experimental and numerical study on the load-bearing capacity, ductility and energy absorption of RC shear walls with opening containing zeolite and silica fume

Mehran Mozafarjazi[a*] and Ramin Rabiee[b]

[a]*PhD student, Department of Civil, Construction, and Environmental Engineering, Marquette University, Milwaukee, WI 53233, USA*
[b]*Assistant Professor, Department of Civil and Environmental Engineering, Ohio Northern University, Ada, OH, USA*

ARTICLE INFO

Article history:
Received 3 October 2023
Accepted 24 January 2024
Available online
24 January 2024

Keywords:
Concrete shear wall
Opening
Silica fume
Zeolite
Ductility
Energy absorption
Load-bearing capacity

ABSTRACT

This article originates from an experimental program and nonlinear finite element analysis aimed at examining how pozzolanic concrete influences the behavior of RC shear walls with openings. To achieve this, stress-strain diagrams, and the elastic modulus of 33 cylindrical concrete specimens, each containing varying percentages of silica fume and zeolite (ranging from 0% to 25%), were evaluated. The impact of silica fume and zeolite pozzolans on the ductility and load-bearing capacity of RC shear walls with openings was explored. This was done by analyzing the mechanical properties of the specimens and integrating them into the analytical model. Subsequently, a shear wall with conventional concrete was simulated using the finite element method (FEM). The study delved into the effects of substituting the initial concrete with pozzolanic concrete within the shear wall. Additionally, it investigated the simultaneous reduction in the diameter of the reinforcing bars employed, all in the pursuit of attaining the optimal design for these walls. The findings demonstrated that employing pozzolanic concrete in shear walls, coupled with a balanced configuration of rebar, led to heightened ductility, improved energy absorption, and an enhanced load-bearing capacity for the walls.

1. Introduction

Structural walls have been usually adopted as the main earthquake-resistant components of reinforced concrete buildings. However, they usually have some openings according to the intention of the architectural design, and the opening ratios, locations, and shapes are often various. Theoretical and experimental research made on ductility and loading capacity of the concrete shear wall with openings. Finite element studies combined with experimental results may be the only alternative to understanding their behaviour. Nowadays, due to the availability of powerful computers, numerical modelling approaches are able to provide an accurate alternative to the experimental investigations of reinforced concrete structural walls (Thomason et al., 2009). Lin and Kuo (1988) and Subedi (1991) conducted finite element analysis and experimental tests to study the ultimate shear strength of concrete shear wall and concluded that the ductility and shear strength of shear wall with an opening are highly affected by reinforcement configuration around the opening, especially diagonal reinforcement. Aguda (1991) studied the behavior and ultimate strength of shear walls with two bands of openings. Results showed that the methods of calculations of concrete walls with one band of opening will be propagated for these specimens. Arabzadeh and Mozafarjazi (2018) developed a non-linear finite element method using concrete damage plasticity model (CDPM) under the monotonic loading and showed that parameters of opening area and position, bands of opening coupling, beam dimensions and diagonal reinforcement have a considerable effect on ultimate load capacity of RC shear walls with opening. Research made by Yanez et al. (1992) were performed on 6 shear walls with different opening dimensions and locations. The experimental modes recorded a ductile failure by reaching the yielding limit of the vertical reinforcement, followed by the crushing of the concrete from the base of the small compressed pier. Kim and Lee (2003), conducted a finite element analysis and experimental

* Corresponding author.
E-mail addresses: mehran.mozafarjazi@marquette.edu (M. Mozafarjazi)

ISSN 2291-8752 (Online) - ISSN 2291-8744 (Print)

doi: 10.5267/j.esm.2024.1.009

work to study the ultimate strength of shear wall with openings under lateral load. They concluded that the load-carrying capacity of the section is not only affected by the width of opening but also affected by the depth of opening as well. Balkaya and Kalkan (2004) compared 2D and 3D nonlinear finite element analysis of concrete shear walls with the opening and concluded that the stress flow, load-bearing capacity and crack patterns around the openings of pierced shear walls observed through the 3D models have more in accordance with experimental results. Warashina et al. (2008) performed an experimental and theoretical analysis to investigate the effect of opening location. He showed that the opening dimension and location could affect the compressed area of the wall. Palermo and Vechioo (2007) worked on FEM analysis of structural walls with openings to develop a simple but rational method of strain distribution and they could simulate behavioural aspects such as ultimate strength, displacements, energy dissipation, and failure mechanisms very well. Guan et al. (2010) and Fragomeni et al. (2012) used the nonlinear Layered Finite Element Method (LFEM) to undertake a comparative study to verify the effectiveness of the method in predicting the failure characteristics of seven two-way normal strength concrete walls without and with window and door openings. The results of this study have assisted in verifying the LEFM as a reliable and effective technique for determining a relationship between ultimate load-bearing capacity and varying opening configurations. Therefore, more dependable design aids and accurate formulas can be established. Wang et al. (2010) and Chowdhury et al. (2012) developed the Strut and Tie model to design concrete shear walls with different opening locations. Marius (2013) did theoretical and experimental studies on structural walls with staggered openings, lamellar walls, and walls with bulbs and investigated degradation of the stiffness, the ductility function to the intensity of the seismic force, the presence of the vertical forces, the position and the size of the openings and different reinforcing figures. The results theoretically obtained with the help of the calculus programs that have been confirmed experimentally. The analysis of the failure modes, obtained with the computing methodology proposed, contributed to the completion of the seismic design codes for shear walls with staggered openings. Husain et al. (2019). proposed some configurations of using CFRP laminates around the openings using FEM and conducted that CFRP laminates substantially increases the lateral load strength and deformation capacity of the shear wall with openings and improves the ductility and energy dissipation of the shear wall. Gonchan et al. (2023) investigated the effect of steel plates on the bearing capacity, ductility, energy dissipation capacity and shear deformation of shear walls with different opening sizes and concluded that pasting steel plates around the openings can effectively restrain the crack at the corner of the opening and improve the integrity of the shear wall.

Mechanical properties of concrete like elastic modulus are key factors to design of RC structures. The elastic modulus of concrete is needed by designers for stiffness and deflections evaluations. Predicting the elastic modulus is also important in reinforced and prestressed concrete for shrinkage and creep evaluation as well as crack control especially at an early age (Mesbah et al., 2002; Khan et al., 1995). Studies have shown (Nassif & Suksawang, 2002; Bouzoubaa et al., 2002; Bilodeau & Malhotra, 2000; Giaccio & Malhotra, 1988) that adding Pozzolans enhances the strength and durability of the concrete. Most of these supplementary cementitious materials are by-products. Thus, their inclusion not only serves as an inestimable means to protect environmental resources but also improves concrete construction properties, including its sustainability (PUB, 1999; Malhotra & Mehta, 1996; Mosoarca, 2014; Mehta & Monteiro, 2014). Najm and Naaman (1995) measured the elastic modulus of High-Performance Fiber Reinforced Cement-based Concrete (HPFRCC) in tension and compression. They concluded that the elastic modulus of a composite material is greatly affected by the range over which it is measured and that the modulus values in compression are less variable than those in tension. Hani et al. (2005) discusses the experimental evaluation of the elastic modulus of high-performance concrete made from mixes using various percentages of fly ash, silica fume, and granulated blast furnace slag. Results are compared to those from control specimens at various ages between 1 and 90 days. The results showed that adding silica fumes resulted in an increase in strength and modulus at early ages; however, there was no change in the modulus at 28 and 56 days. In addition, adding 20% fly ash with various percentages of silica fume had an adverse effect on both strength and modulus values at all ages to 90 days. Sarıdemir (2014) presents the results of an experimental study on compressive strength and secant elastic modulus of high strength concrete (HSC) containing different levels of silica fume, ground pumice, and silica fume together with ground pumice. He finally showed that artificial intelligent methods have strong potential and can be applied for the prediction of the compressive strength of concrete containing fly ash with different specimen size and shape. Some researchers also investigate the effect of pozzolans on mechanical properties of recycled aggregate concrete. Li et al. (2023) showed that using 10% SF content in geopolymeric recycled aggregate concrete (GRAC) is recommended to improve the mechanical properties of this type of concrete.

In this paper, initially, the mechanical properties and stress-strain curves of 33 cylindrical experimental specimens of normal concrete (without pozzolan) and containing different percentages of silica fume and zeolite are obtained. Subsequently, the mechanical properties and behavioral models of these specimens are used in RC shear walls that are created by using finite element method (FEM) to assess the influence of using these pozzolans on the load-bearing capacity, ductility and energy absorption of these walls. FEM which is used in this paper is verified by experimental results of Aguda et al. (1991).

2.Material characteristics

The materials used throughout this study were type II Portland cement as its chemical properties are given in Table1. Natural river sand with bulk specific gravity of 2.5 and water absorption of 4.3%, coarse aggregate with a maximum size of 10 mm and bulk specific gravity of 2.5, green color zeolite (Z) with fineness of 11000 m2/kg at replacement levels of 0%, 10%, 15%, 20% and 25% is used. Silica fume (SF) with Blaine's fineness of 21000 m^2/kg was used at replacement levels of

0%, 5%, 10%, 15%, 20% and 25%. Chemical analysis of zeolite and Silica fumes are also presented in **Table 1**. The superplasticizer used was based on poly carboxylic ether with yellow marble color.

Table 1. Chemical properties of binders

Constituents (% by mass)	Type II Cement	Zeolite	Silica fume
SiO_2	39.8	54	94
Al_2O_3	6.2	46	1.3
Fe_2O_3	3.9	1.2	0.7
MgO	0.18	0.03	0.3
CaO	64.5	0.09	0.1
Na_2O	0.18	0.1	0.2
L.O.I	1.53	1.5	2.1

3. Experimental work

In this study, 33 cylindrical concrete specimens with perimeter and height of 150*300 mm were made in the lab, which 3 specimens were without pozzolans (control sample) and 30 specimens contained 5,10,15,20 and 25 % of silica fume and zeolite. The compressive strength and stress-strain diagram tests are developed in accordance with ASTM C-39 (2014). The mix proportions of control concrete (OC), concrete with silica fume (CS) and concrete with zeolite (CZ) are shown in **Table 2**.

Table 2. Mix proportion of the substrate concrete (kg/m3)

Type	Specimen	Cement (Kg/m^3)	Water (Kg/m^3)	Coarse aggregate (Kg/m^3)	River sand (Kg/m^3)	Superplasticizer (Kg/m^3)	Silica fume (Kg/m^3)	Zeolite (Kg/m^3)
OC	OC	400	150	٨٧٧	980	1.7	----	----
CS	CS1	380	150	877	980	1.7	20	----
	CS2	360	150	877	980	1.8	40	----
	CS3	340	150	877	980	1.8	60	----
	CS4	320	150	877	980	1.9	80	----
	CS5	300	150	877	980	2	100	----
CZ	CZ1	380	150	877	980	1.7	----	20
	CZ2	360	150	877	980	1.9	----	40
	CZ3	340	150	877	980	1.9	----	60
	CZ4	320	150	877	980	2	----	80
	CZ5	300	150	877	980	2.2	----	100

After one day, the specimens were evicted from molds and have been cured for 28 days. Finally, the compressive strength of specimens was measured to obtain stress-strain curves and elastic modulus of the samples that was calculated by ASTM C-39 (2014).

3.1 Experimental results

The results of calculated elastic modulus obtained from experimental work are presented in **Fig. 1** and **Fig. 2**. The figures show an increasing percentage of elastic modulus of concrete pozzolan by increasing the percentage of silica fume (E_{SF}) and zeolite (E_Z) pozzolans. Horizontal axis represents the ratio of the used pozzolan to the total used cement of the control specimen and the vertical axis shows the elastic modulus of each sample to control the concrete (E_0). As can be seen in **Fig. 1** and **Fig. 2**, by increasing 25% silica fume and 20% zeolite instead of using cement in control concrete, elastic modulus of the specimens enhance 1.8 and 0.5 times more than elastic modulus of normal concrete. It is also shown that 20% increase or decrease in the amount of zeolite, leads to reduction in elastic modulus of the specimens. Maximum elastic modulus of normal and pozzolanic concrete are shown in **Table 3**.

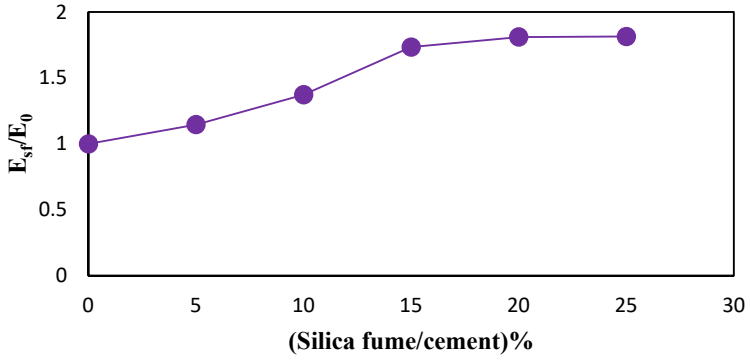

Fig. 1. Changing rate of elastic modulus of concrete for different percentages of SF.

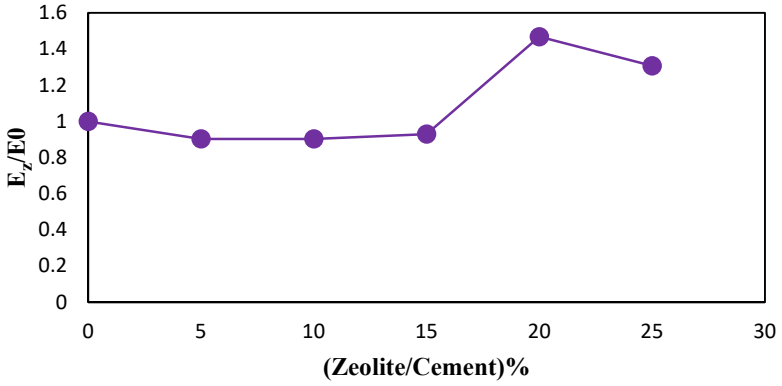

Fig. 2. Changing rate of elastic modulus of concrete for different percentages of Z.

Table 3. Comparison Of maximum Elastic modulus of the experimental specimens

Specimen	Elastic modulus (Gpa)
OC	29.34
CS5	44.48
CZ4	36.78

4.Verification

In 1991, two scaled six stories concrete shear walls with two bands of openings were tested by Aguda (1991) in Dundee University. In this paper, Agudas' wall was modelled in the FE program to verify the developed FEM and analytical results were compared with experimental outputs. The dimensions of the wall and reinforcement details are presented in **Fig. 3** and **Fig. 4**, respectively.

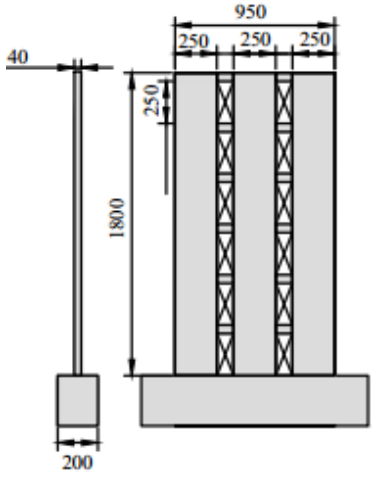

Fig. 3. Experimental Agudas' wall.

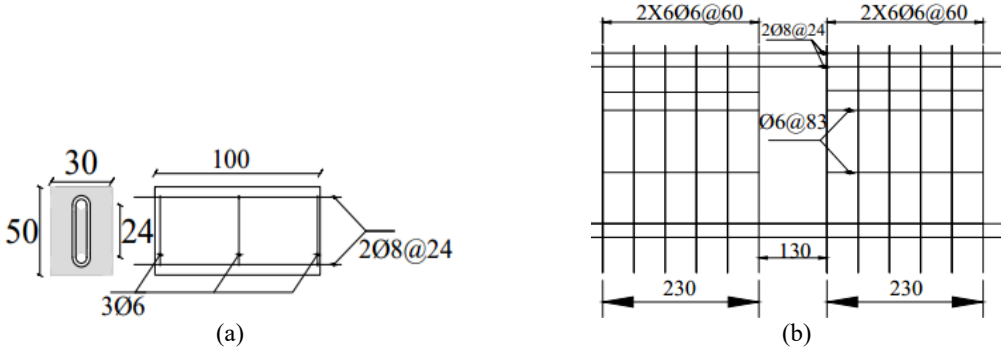

Fig. 4. (a) Reinforcement detail of coupling beam. (b) Reinforcement detail of piers.

4.1. Numerical Analysis

In order to simulate the mechanical behaviour of structural walls, a numerical analysis was carried out, using a three dimensional nonlinear FEM. The FEM employs eight node quadrilateral isoperimetric elements with nine gauss points. The mechanical properties of the reinforcement tie were determined in accordance with the original macro model by Belarbi and Hsu (1994) have been shown in **Fig. 5-a**. However, the compressive concrete model is considered based on the Maekawa model (2004) and is presented in **Fig. 5-b**.

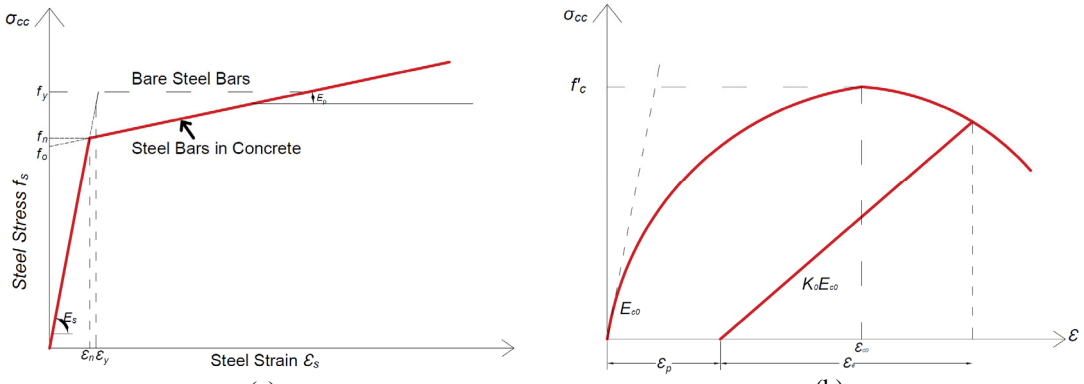

(a) (b)

Fig. 5. (a) Belarbi and Su reinforcement model. **(b)** Maekawa compressive model.

where E_{c0}= initial stiffness; K_0 =fracture parameter; E_0 coefficient=2; ε_{c0}=uniaxial strain at uniaxial compressive strength (f'_c); f_y= reinforcement yield strength; ε_y= uniaxial strain at yield strength; E_s= elastic modulus of reinforcement. One of the effective factors on the response of reinforced concrete structures is the tension-stiffening phenomenon. This phenomenon is caused by cohesive stress transfer from rebar to concrete and thus decreases the strain of rebars between the cracks. Moreover, it has a significant impact on the deformation and crack width of reinforced concrete elements. To correct the effect of tension stiffening in this paper, Shima et al. (1987) model is used as follows:

$$\sigma_{\mathrm{t}} = f_t \left(\frac{\varepsilon_{tu}}{\varepsilon_t}\right)^c \tag{1}$$

where f_t = concrete tensile strength; ε_t = strain concrete; ε_{tu} = the strain corresponding to concrete tensile strength and c is the variable of the model that is 0.4 for threaded rebar and is equal to 0.3 for welded steel mesh. Vechioo and Collins (1996 & 1993) tested 30 reinforced concrete panels and modelled them by compression field theory and found that tensile stress causes some cracks in one direction and this tensile in normal direction cracks the specimens that have a softer compressive behaviour than the uniaxial compression test. This phenomenon is called compression softening due to lateral cracks and is modified by softening factor in the FEM as follows:

$$\beta = \frac{1}{0.8 - 0.34\dfrac{\varepsilon_1}{\varepsilon_0}} \tag{2}$$

where the ε_1 is principal tensile strain and ε_0 is the corresponding strain to compressive strength of concrete.

4.2. Comparison of experimental results and FEM analysis

In this part, Agudas' wall is modelled in FEM by using foresaid constitutive laws. Boundary conditions are considered by modelling the foundation.

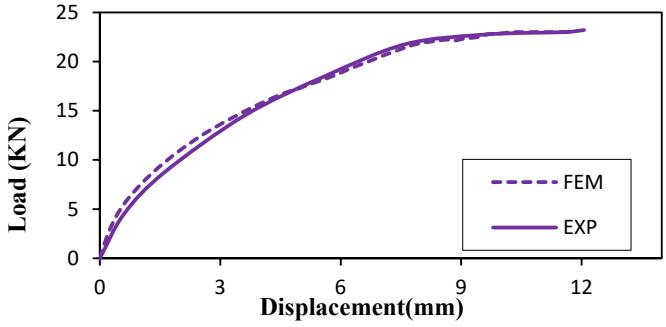

Fig. 6. Load Displacement diagrams of experimental wall and FEM analysis.

Loading of the wall is applied by the displacement of a rigid steel plate attached to the right upper corner of it. Applied displacement by rigid steel plate prevents stress concentration and crushing of concrete in this part of the wall. Load displacement diagrams of the analytical and experimental results of the Agudas' wall are presented in **Fig. 6**. As can be seen, the results of the FEM is coincided with high accuracy on experimental results. The failure mechanism of the wall is shown in **Fig.7** in both FEM analysis and experimental conditions. The wall has a flexure failure mechanism in both manners. Additionally, as can be seen in figures, coupling beams withstand large deformations before failure and thus the main parts of the wall experience less damage. Coincidence of failure mechanisms in experimental and analytical conditions show that the FEM can appropriately model the behaviour of concrete shear walls.

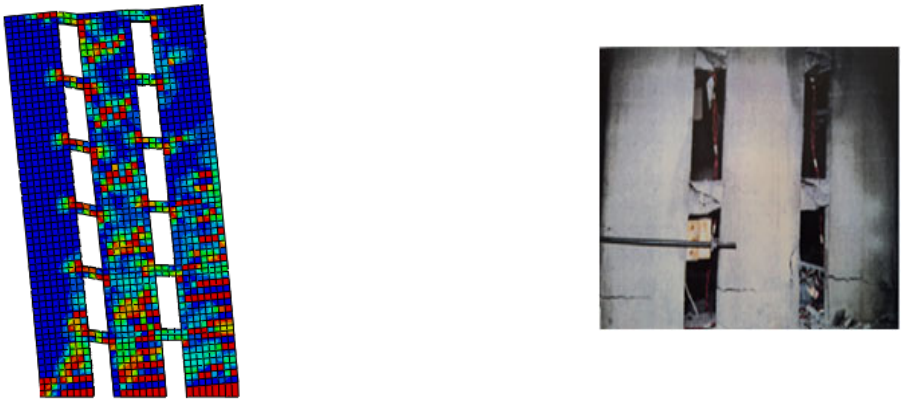

(a) (b)

Fig. 7. (a) FEM failure mechanism. (b) experimental failure mechanism (1991)

5. Parametric Study

To begin, the first step is to design a concrete shear wall using normal concrete (referred to as the OC specimen) in accordance with the ACI 318-18 code (2018). The wall includes a 1000*1000mm opening and is then modeled using the Finite Element Method (FEM), as illustrated in Figure 8 (referred to as the WCO wall). Subsequently, we aim to explore the impact of pozzolanic concrete by incorporating it in two different variations: CS5 and CZ4 specimens. As a result, this prompts the reconfiguration of the WCS and WCZ walls, respectively. The main objective is to examine how the introduction of pozzolans influences the load-bearing capacity, ductility, and energy absorption of these specimens. Finally, we present an economically viable design that attains sufficient ductility by reducing the diameter of the rebars employed within the wall. It is essential to note that the dimensions of the opening and the arrangement of reinforcement remain consistent across all modeled walls. The loading conditions applied to the numerical models mirror those utilized in the experimental conditions.

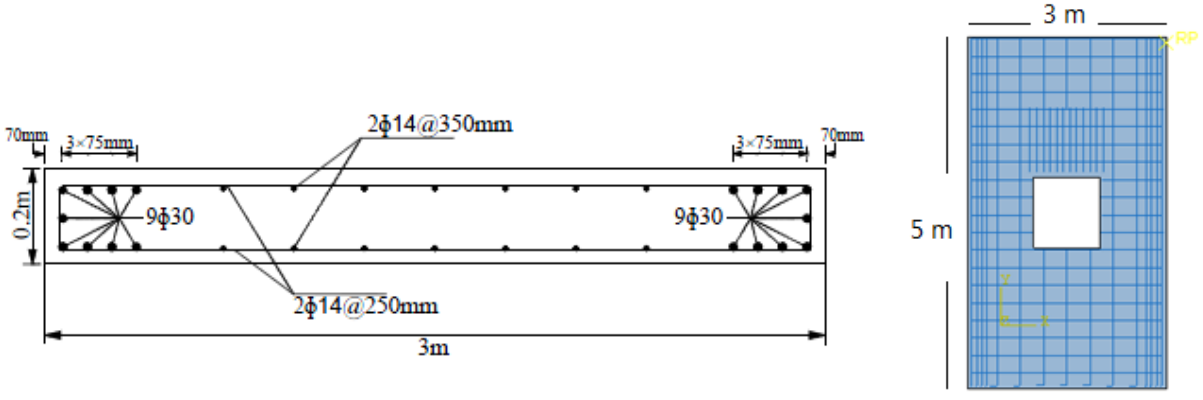

(a) (b)

Fig. 8. (a) Plan reinforcement detail of modelled wall. (b) Configuration of reinforcing and dimension of the modelled wall.

6. Result and Discussion

The Load-displacement diagrams depicting the behavior of the analyzed walls are presented in **Fig. 9**. From these diagrams, it becomes evident that an increase in the amount of f'c, attributed to the presence of silica fumes, leads to a more pronounced ascending rate in the linear portion compared to the other walls.

Furthermore, the load-bearing capacity of the WCS wall surpasses that of the WCO and WCZ walls by 30.5% and 14.5%, respectively. The introduction of silica fumes within the WCS model results in the maximum stress at the furthest compressive fiber exceeding 0.5f'c. This imparts to it a more elastoplastic behavior in contrast to the other walls. The diagrams also indicate that the WCS wall attains its maximum tensile strength in the furthest tensile fiber much earlier than the other walls, leading to a non-linear stress redistribution across a limited section of the cross-section. Moreover, the initiation of cracking occurs in the tension area of the wall.

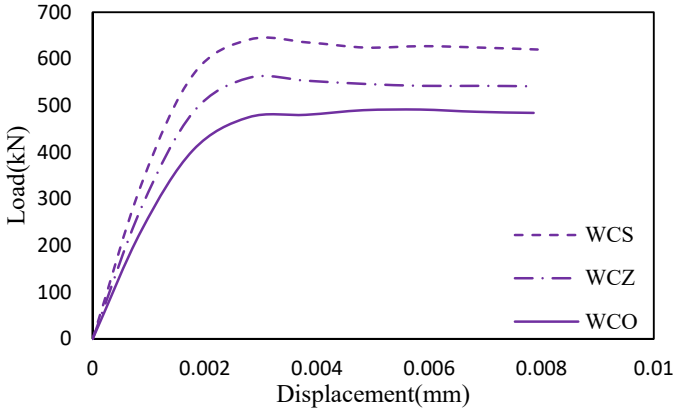

Fig. 9 Load-displacement of modeled walls.

Fig.10 illustrates the failure mechanism observed in the modeled walls. It is evident that flexural failure has taken place within the walls. Initially, as the width, length, and number of cracks stabilize in the tension area of the wall, fresh cracks emerge in the compression area. Ultimately, a plastic hinge forms at the base of the wall. The presence of an opening in the wall results in stress concentration at the marginal regions of the opening, prompting the appearance of new cracks that propagate at a 45-degree angle.

The utilization of silica fume and zeolite pozzolans in the WCZ and WCS walls leads to a reduction in the number of cracks and the size of the plastic hinge. This reduction in damage results in a higher ultimate load-bearing capacity for the WCS wall.

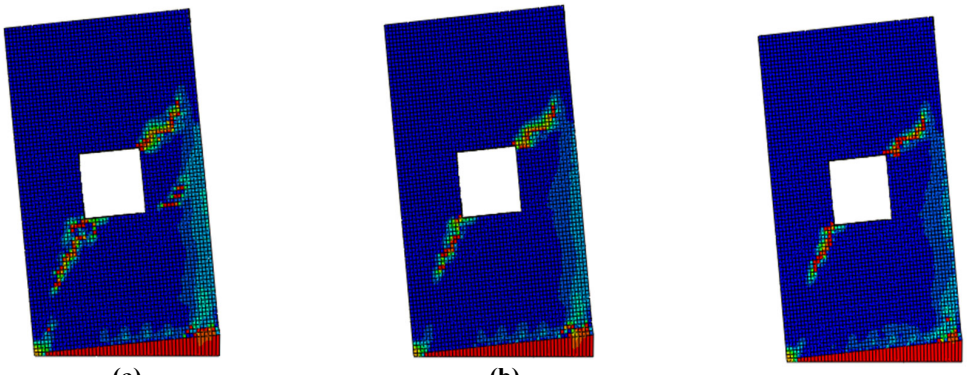

Fig. 10. Failure mechanisms of modeled walls (a): WCO (b): WCZ (c): WCS.

The Strain-stress curves of the modeled walls are displayed in **Fig. 11**. According to these curves, the behavior of the walls varies depending on the type of concrete employed; however, all the curves exhibit a similar overall trend of expansion. Across all three modeled walls, as the stress-strain curve approaches 30% of the ultimate strength, there is an increase in the width, length, and number of cracks in the interfacial transition zone (ITZ). Comparatively, the WCS wall demonstrates an ultimate strength 34% higher than that of the WCO wall and 68% higher than the WCZ wall. Notably, the initial slope of the WCS curve surpasses that of the other walls. Furthermore, the ultimate strain of the WCS wall slightly exceeds that of the other two walls. This can be attributed to the elevated tensile strength of the WCS wall, which consequently leads to a reduction in the height of the compressive area in the stress diagram. This reduction contributes to a decline in the equilibrium state.

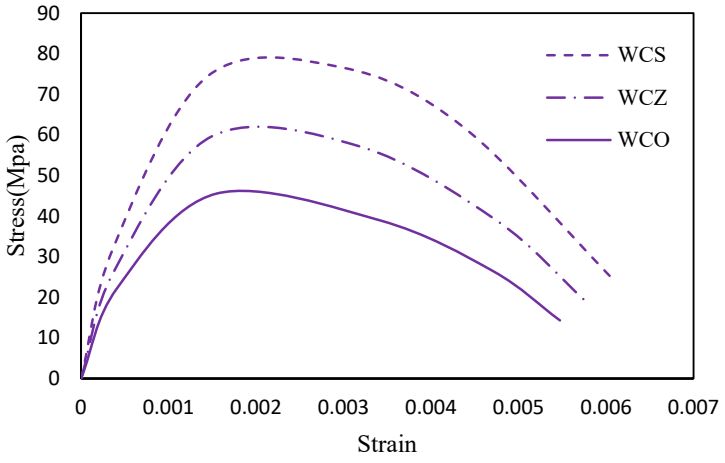

Fig. 11. Stress Strain diagrams of modeled walls.

Ductility is defined as a crucial property in achieving the acceptance of pozzolanic concrete structures in practice. Three parameters, namely yield displacement Δ_y, ultimate displacement Δ_u and displacement ductility ratio μ, were taken into consideration to evaluate the displacement ductility index. In present study, yield displacement (Δ_y) corresponding to the load at yielding was evaluated according to the method reported by Park (1989). The ultimate displacement (Δ_u) was defined as displacement corresponding to 85% of peak load on the descending branch of the envelope curve. The ductility index μ was defined as $\mu = \Delta_u/\Delta_y$. As shown in **Table 4**, the displacement ductility ratios of specimens WCS and WCZ were 33 and 26% higher than that of reference specimen WCO, respectively.

Energy dissipation is described as a basic structural property of RC members when subjected to seismic loads. According to Nguyen-Minh et al. (2018), the energy absorption capacity (*E*b) was estimated by calculating the area under the load–displacement curves until the maximum loads. Table 4 shows that the final dissipated energy absorption capacity of specimens WCS and WCZ was 36 and 18% higher than that of reference specimen WCO, respectively. Energy dissipation is a fundamental structural property of reinforced concrete (RC) members under seismic loads. Nguyen-Minh et al. (2018) proposed estimating the energy absorption capacity (Eb) by calculating the area under the load-displacement curves up to the maximum loads. As presented in **Table 4**, specimens WCS and WCZ exhibited final dissipated energy absorption capacities 36% and 18% higher than the reference specimen WCO, respectively.

Table 4. Load capacity, ductility, energy absorption and failure modes of wall specimens

Wall Specimen	Peak load (KN)	Energy absorption capacity (KNmm)	Ductility index $\mu=\Delta_u/\Delta_y$	Failure mode
OC	485	3176	3.12	Flexure
CS5	640	4315	4.11	Flexure
CZ4	550	3740	3.9	Flexure

7. Conclusions

1- The utilization of Silica fume and zeolite pozzolans yields a notable enhancement in the elastic modulus and compressive strength when contrasted with regular concrete. Significantly, Silica fume exerts a more profound impact on augmenting concrete properties compared to zeolite.

2- As evident, the presence of openings in the reinforced concrete shear walls leads to a reduction in load-bearing capacity, ductility, and energy dissipation of these specimens. The use of pozzolanic concrete, especially silica fume, can enhance the aforementioned properties in RC shear walls with openings and reduction of the diameter of the used rebars simultaneously.

3- The application of Silica fume pozzolan propels a remarkable advancement in load-bearing capacity, ductility and energy absorption of the wall, a superiority evident when compared to the effects of zeolite.

4- In the pursuit of designing a concrete shear wall with high strength and ductility, an appropriate approach involves leveraging Pozzolans to amplify the concrete's modulus of elasticity while concurrently optimizing the configuration by reducing the diameter of bending rebars to an optimal level.

5- According to the failure mechanism of the modelled walls and the substantial reduction in crack propagation and deformation encircling bending rebars, the profound efficacy of this type of rebar becomes vividly apparent in comparison to shear reinforcement.

References

ACI Committee. (2018). Building code requirements for structural concrete (ACI 318-05) and commentary (ACI 318R-05). American Concrete Institute.

Aguda, G. O. (1991). *Ultimate Strength Tests for RC Coupled Shear Walls with Two Bands of Openings* (Doctoral dissertation, University of Dundee).

Arabzadeh, A., & Mozafarjazi, M. (2018). Effective Parameters on Behavior and Load Capacity of Concrete Shear Wall with Regular Opening. *Amirkabir Journal of Civil Engineering*, *50*(3), 421-432.

ASTM International Committee C09 on Concrete and Concrete Aggregates. (2014). *Standard test method for compressive strength of cylindrical concrete specimens*. ASTM international.

Balkaya, C., & Kalkan, E. (2004). Three-dimensional effects on openings of laterally loaded pierced shear walls. *Journal of structural engineering*, *130*(10), 1506-1514.

Belarbi, A., & Hsu, T. T. (1994). Constitutive laws of concrete in tension and reinforcing bars stiffened by concrete. *Structural Journal*, *91*(4), 465-474.

Bilodeau, A., & Malhotra, V. M. (2000). High-volume fly ash system: concrete solution for sustainable development. *Materials Journal*, *97*(1), 41-48.

Bouzoubaa, N., Fournier, B., Malhotra, V. M., & Golden, D. M. (2002). Mechanical properties and durability of concrete made with high-volume fly ash blended cement produced in cement plant. *Materials Journal*, *99*(6), 560-567.

Chowdhury, S. R., Rahman, M. A., Islam, M. J., & Das, A. K. (2012). Effects of openings in shear wall on seismic response of structures. *International Journal of Computer Applications*, *59*(1).

Fragomeni, S., Doh, J. H., & Lee, D. J. (2012). Behavior of axially loaded concrete wall panels with openings: an experimental study. *Advances in structural engineering*, *15*(8), 1345-1358.

Giaccio, G. M., & Malhotra, V. M. (1988). Concrete incorporating high volumes of ASTM Class F fly ash. *Cement, Concrete, and Aggregates*, *10*(2), 88-95.

Guan, H., Cooper, C., & Lee, D. J. (2010). Ultimate strength analysis of normal and high strength concrete wall panels with varying opening configurations. *Engineering Structures*, *32*(5), 1341-1355.

Husain, M., Eisa, A. S., & Hegazy, M. M. (2019). Strengthening of reinforced concrete shear walls with openings using carbon fiber-reinforced polymers. *International Journal of Advanced Structural Engineering*, *11*, 129-150.

Khan, A. A., Cook, W. D., & Mitchell, D. (1995). Early age compressive stress-strain properties of low-, medium, and high-strength concretes. *Materials Journal*, *92*(6), 617-624.

Kim, H. S., & Lee, D. G. (2003). Analysis of shear wall with openings using super elements. *Engineering Structures*, *25*(8), 981-991.

Li, B., Gao, A., Li, Y., Xiao, H., Chen, N., Xia, D., ... & Li, C. (2023). Effect of silica fume content on the mechanical strengths, compressive stress–strain behavior and microstructures of geopolymeric recycled aggregate concrete. *Construction and Building Materials*, *384*, 131417.

Li, G., Liu, M., Pan, Z., Lu, L., & Yuan, G. (2023, May). Strengthening effect of steel plates on seismic behaviors of RC shear walls with various size post-openings. In *Structures* (Vol. 51, pp. 814-827). Elsevier.

Lin, C. Y., & Kuo, C. L. (1988, August). Behavior of shear wall with Opening. In *Proceedings of Ninth world Conference on Earthquake Engineering. Tokyo-Kyoto, Japan, IV* (pp. 535-540).

Maekawa, K., Okamura, H., & Pimanmas, A. (2003). *Non-linear mechanics of reinforced concrete*. CRC Press.

Malhotra, V. M., & Mehta, P. K. (1996). 'Pozzolanic and Cementitious Materials, Gordon and breach publishers, advances in concrete. *technology, ISSN1024-5038*, *1*.

Mehta, P. K., & Monteiro, P. J. (2014). *Concrete: microstructure, properties, and materials*. McGraw-Hill Education.

Mesbah, H. A., Lachemi, M., & Aitcin, P. C. (2002). Determination of elastic properties of high-performance concrete at early ages. *Materials Journal*, *99*(1), 37-41.

Marius, M. (2013). Seismic behaviour of reinforced concrete shear walls with regular and staggered openings after the strong earthquakes between 2009 and 2011. *Engineering Failure Analysis*, *34*, 537-565.

Mosoarca, M. (2014). Failure analysis of RC shear walls with staggered openings under seismic loads. *Engineering Failure Analysis*, *41*, 48-64.

Najm, H. S., & Naaman, A. E. (1995). Prediction Model for the Elastic Modulus of High-Performance Fiber Reinforced Cement-Based Composites. *Materials Journal*, *92*(3), 304-314.

Nassif, H. H., Najm, H., & Suksawang, N. (2005). Effect of pozzolanic materials and curing methods on the elastic modulus of HPC. *Cement and Concrete Composites*, *27*(6), 661-670.

Nassif, H., & Suksawang, N. (2002). Effect of curing methods on durability of high-performance concrete. *Transportation research record*, *1798*(1), 31-38.

Palermo, D., & Vecchio, F. J. (2007). Simulation of cyclically loaded concrete structures based on the finite-element method. *Journal of Structural Engineering*, *133*(5), 728-738.

PUB, V. (1999). High performance concrete.

Sarıdemir, M. (2014). Effect of specimen size and shape on compressive strength of concrete containing fly ash: Application of genetic programming for design. *Materials & Design (1980-2015)*, *56*, 297-304.

Shima, H., Chou, L. L., & Okamura, H. (1987). Micro and macro models for bond in reinforced concrete. *Journal of the Faculty of Engineering*, *39*(2), 133-194.

Subedi, N. K. (1991). RC-coupled shear wall structures. I: Analysis of coupling beams. *Journal of Structural Engineering*, *117*(3), 667-680.

Thomson, E. D., Perdomo, M. E., Picón, R., Marante, M. E., & Flórez-López, J. (2009). Simplified model for damage in squat RC shear walls. *Engineering Structures*, *31*(10), 2215-2223.

Vecchio, F. J., & Collins, M. P. (1986). The modified compression-field theory for reinforced concrete elements subjected to shear. *ACI J.*, *83*(2), 219-231.

Vecchio, F. J., & Collins, M. P. (1993). Compression response of cracked reinforced concrete. *Journal of structural engineering*, *119*(12), 3590-3610.

Wang, J. Y., Sakashita, M., Kono, S., Tanaka, H., & Lou, W. J. (2010). Behavior of reinforced concrete structural walls with various opening locations: experiments and macro model. *Journal of Zhejiang University SCIENCE A*, *11*(3), 202-211.

Warashina, M., Kono, S., Sakashita, M., & Tanaka, H. (2008, October). Shear behavior of multi-story RC structural walls with eccentric openings. In *The 14th world conference on earthquake engineering, Beijing, China* (pp. S15-029).

Yanez, F. V., Park, R., & Paulay, T. (1992, July). Seismic behaviour of walls with irregular openings. In *Earthquake Engineering. Tenth World Conference, Balkema, Rotterdam*.